Original papers

PIEZO2 promotes cell proliferation and metastasis in colon carcinoma through the *SLIT2/ROBO1/VEGFC* pathway

*Haotian Shang[C], *Aiguo Xu[B,C], Haicui Yan[B], Dandan Xu[B,C], Jingyu Zhang[A,C,D,F], Xinjian Fang[E,F]

Department of Oncology, Lianyungang No. 2 People's Hospital, Lianyungang Clinical College of Bengbu Medical College, China

A – research concept and design; B – collection and/or assembly of data; C – data analysis and interpretation;
D – writing the article; E – critical revision of the article; F – final approval of the article

Address for correspondence
Jingyu Zhang
E-mail: lygzjy2013@outlook.com

Abstract

Background. The *PIEZO2* may be involved in the occurrence and development of tumors.

Objectives. To explore the potential mechanism and effect of *PIEZO2* on colon cancer.

Materials and methods. We assessed the expression and prognostic role of *PIEZO2* in patients with colon cancer. The role of *PIEZO2* in SW480 cell proliferation, migration and invasion in vitro was investigated using cell counting kit-8 (CCK-8), wound healing, and transwell and cell invasion assays, respectively. The effect of *PIEZO2* on SW480 cells in vivo was also explored. The potential mechanisms of *PIEZO2* in SW480 cells were detected using quantitative reverse-transcription polymerase chain reaction (qRT-PCR) and western blot.

Results. The *PIEZO2* was significantly increased in colon cancer tissues and the *PIEZO2* high expression group was associated with a lower overall survival (OS) rate. Furthermore, *PIEZO2* knockdown weakened the proliferation, migration and invasion of SW480 cells. The *PIEZO2* knockdown was related to a lower expression of *SLIT2*, *ROBO1*, *HIF-1a*, and *VEGFC*. Finally, the tumors in control SW480 cells grew faster and larger than those in mice inoculated with si-*PIEZO2* SW480 cells. Moreover, the si-*PIEZO2* SW480 cell group showed a reduced expression of *Ki67* and *VEGFC* and, at the same time, a significantly higher apoptosis index of tumor cells compared to the control group. The expression of *PIEZO2* was higher in cancer-associated fibroblasts (CAFs) of colon cancer.

Conclusions. The *PIEZO2* was increased in colon cancer tissues and was an unfavorable gene in patients with colon cancer, promoting colon cell proliferation, migration and invasion through the *SLIT2/ROBO1/VEGFC* pathway.

Key words: colon cancer, cancer-associated fibroblasts, *PIEZO2*, *SLIT2/ROBO1/VEGFC* pathway

Background

Because of its high mortality rate, colorectal cancer (CRC) has become a major health burden worldwide. Globally, there were more than 1.9 million new CRC cases and 935,000 deaths reported in 2020.[1] If the cancer is local, 90% of patients with CRC survive 5 years after the diagnosis. However, once the disease has distant metastases, this rate reduces dramatically to 10%.[2] The genetics of cancer cells is not a sole factor influencing tumor metastasis; additionally, the interaction between tumor cells and the surrounding microenvironment plays a pivotal role in tumor differentiation and progression.[3] Mechanical stimulation including stiffness, shear stress, compression, and tensional forces from the surrounding microenvironment is frequent in tumor cells.[4] Mechanotransduction, the conversion of physical stimuli into biochemical or electrical signals, plays a key role in biological processes in tumor cells, including development, proliferation, migration, and apoptosis.[5]

The *PIEZO* transmembrane proteins are conserved ion-channel proteins that sense external mechanical forces. The cell membrane pressure induced by external mechanical force can regulate changes in intracellular ions and exert physiological effects by changing the closure of the *PIEZO* transmembrane protein. The *PIEZOs* can regulate nociception and stem cell differentiation in *Drosophila*. The *PIEZO* transmembrane proteins mainly include 2 homologous proteins: *PIEZO1* and *PIEZO2*. Although these proteins are homologous, their roles reported in the literature are not consistent. The *PIEZO1* is mainly distributed in endothelial cells, red blood cells and hair cells in cochlea, as well as kidney, bladder and lung cancer cells. Under normal physiological conditions, *PIEZO1* is primarily responsible for the regulation of intravascular balance, blood pressure and axon growth. The *PIEZO2* is mainly distributed in the dorsal root nerve and trigeminal ganglion, which are responsible for regulating touch, proprioception of muscles and airway extension. It has been reported that *PIEZOs* are involved in the formation of human blood vessels.[6] The *PIEZO* knockout can affect the growth and development of mice. Because of the important role of *PIEZOs*, the functions of the 2 homologous proteins have been increasingly studied.

In recent years, many studies have reported that *PIEZOs* may be involved in the occurrence and development of tumors, and may be related to angiogenesis. Gottlieb et al. reported that the reduction or deletion of *PIEZO1* played an important role in lung cancer metastasis,[7] while Yang et al. indicated that the decrease in *PIEZO1* expression was related to the decrease in the gastric cancer metastasis.[8] A study by Yang et al. showed that *PIEZO2* knockout can reduce angiogenesis, vascular permeability, endothelial cell proliferation, metastasis, and tubule formation in gliomas.[9] Another study showed that the expression of *PIEZO1/2* was different in bladder cancer formation, suggesting that *PIEZO1/2* plays a role in the proliferation and angiogenesis of bladder cancer cells.[10] Chen et al. reported that the expression of *PIEZO1* was inversely proportional to the stage and prognosis of glioma.[11] The *PIEZO1* can regulate changes in the extracellular matrix and tissue hardness as well as promote tumor progression by activating the integrin focal adhesion kinase (*FAK*) signaling pathway; however, *PIEZO2* is not a prognostic factor. In a study by Pardo-Pastor et al., it was shown that *PIEZO1* mainly forms a mechanoreceptor ion pathway in breast cancer cells, whereas *PIEZO2* is involved in regulating RhoA, actin skeleton formation and cell movement.[12] However, the roles of *PIEZOs* in colon cancer and their underlying mechanisms remain unclear and need to be further elucidated.

Previous studies showed that the *SLIT/ROBO* signaling pathway inhibited the migration of nerve cells in the central nervous system, prevented the nerve axon at the suture from passing through the middle line of the nerve tube, and controlled the accurate localization of neurite in nervous system. Studies on the expression and function of *SLIT/ROBO* signaling in various cancers have been conducted.[13–15] Recently, the molecular mechanism of *SLIT2/ROBO1* signaling in the regulation of colon cancer tumorigenesis has also been deeply studied. The *SLIT2* was highly expressed in colon cancer and its expression increased in pathological stages.[16] At the same time, *SLIT2/ROBO1* signaling induced tumor metastasis in colon cancer partially through the activation of the transforming growth factor beta *(TGF-β)/Smads* pathway. Moreover, *SLIT2/ROBO1* signaling recruited *Src* to *E-cadherin* for tyrosine phosphorylation, leading to *E-cadherin* degradation and epithelial–mesenchymal transition in colon cancer.[17] Accordingly, *SLIT2/ROBO1* signaling played an important role in the formation and metastasis of colon cancer.

Objectives

The above studies suggested *PIEZO2* played an important role in the occurrence and progression of tumors. However, the detailed mechanism was not clear in colon cancer. Therefore, this study was designed to explore the prognostic role of *PIEZO2* in colon cancer and whether the *SLIT2/ROBO1* pathway is responsible for *PIEZO2*-induced progression of colon cancer.

Materials and methods

Patient information

A total of 74 colon cancer tissue samples were collected from January 2015 to December 2016 from patients with colon cancer who received surgery at the Department

of Gastrointestinal Surgery, affiliated with Second People's Hospital of Lianyungang (Bengbu Medical College, China). In addition, we collected 30 colon cancer tumor tissues and matched normal tissues. Clinical data were complete and the last follow-up time was December 2021. Patients included in the study did not receive anticancer therapy such as radiotherapy, chemotherapy or biological therapy before surgery. This study was approved by the Animal Care and Use Ethics Committee of the Affiliated Lianyungang Hospital (Bengbu Medical College, China; approval No. 2020-013-02).

Cell culture

The human colorectal cell line SW480 was purchased from the cell bank of the Chinese Academy of Sciences (Shanghai, China). The cell line grew in Roswell Park Memorial Institute (RPMI) 1640 medium (cat. No. 21870076; Thermo Fisher Scientific, Waltham, USA) supplemented with 10% fetal bovine serum (FBS) (item code: 13011-8611; SolelyBio, Shanghai, China) and cultured in a humidified 5% CO_2 environment at 37°C.

Cell transfection

The SW480 cells were transfected with small interfering (si)RNA targeting *PIEZO2* (si-*PIEZO2*, 5'-GGATAGT-GAAGAGGAGGAAGA-3') and the corresponding negative control (NC) using Lipofectamine™ 2000 Transfection Reagent (1 µL/50 µL, cat. No. 12566014; Invitrogen, Carlsbad, USA). The transfection effect was evaluated using quantitative reverse-transcription polymerase chain reaction (qRT-PCR) and the positive cell line was used for the following experiments.

RT-qPCR assay

Total RNA was extracted using TRIzol reagent (cat. No. 15596026; Invitrogen) and synthesized into cDNA using a reverse transcriptase Moloney Murine Leukemia Virus (M-MLV) Kit (cat. No. 18057018; Invitrogen). The gene expression was detected with a SYBR® Premix Ex Taq™ (cat. No. 11780200; Thermo Fisher Scientific). The primers used in this study are presented in Table 1. The expression of *PIEZO2*, *HIF-1α*, *SLIT2*, *VEGFA*, *VEGFB*, *VEGFC*, *VEGFD*, and *ROBO1* was calculated using the $2^{-\Delta\Delta Cq}$ method, and every value was measured thrice independently. The reaction conditions were as follows: 5 min at 95°C, followed by 40 cycles at 95°C for 30 s and 60°C for 45 s, and a final step at 72°C for 30 min.

Cell counting kit-8 assay

Cells (1×10^4 cells) were plated in four 96-well plates. At every time point, we added 10 µL of cell counting kit-8 (CCK-8) solution (cat. No. C0037; Beyotime Biotechnology,

Table 1. Primer sequences used in the study

Gene symbol	Primer sequence (5'→3')
PIEZO2	forward: TTCCGATACAATGGGCTCTC
	reverse: GAGCTTCAAGGCTCACCAAC
HIF-1α	forward: AGCACAGTTACAGTATTCCAGCAG
	reverse: AGTGGTGGCAGTGGTAGTGG
SLIT2	forward: TCCCCACAAATCTTCCAGAG
	reverse: AGCGTAGTCCTTGGAAAGCA
VEGFA	forward: GAGCGAGAAAGCATTTGTTTG
	reverse: GCAACGCGAGTCTGTGTGTTTT
VEGFB	forward: CAAGGCTGCCATCCAACAA
	reverse: AGGTGGTTAAAATCTGAGTCGGG
VEGFC	forward: ACCAAACAAGGAGCTGGATG
	reverse: TCCCCACAAATCTTCCAGAG
VEGFD	forward: TGTACAGACAGTGGGCAGTGGT
	reverse: AACCTGAAGCTGCCCTGATCT
ROBO1	forward: ACTCCTTACGCCACCACTCAG
	reverse: CCTGTGTTCTGGTCGTATGATTGG
h-actin	forward: TGGACTTCGAGCAAGAGATG
	reverse: GAAGGAAGGCTGGAAGAGTG

Beijing, China) to each well and after the solution was incubated with cells at 37°C for 30 min, the absorbance at 450 nm was measured with a microplate reader. Every experiment was repeated thrice independently.

Wound healing assay

Cells (1×10^5 cells) were seeded in 12-well plates. When cells reached 80% confluence, a 10-microliter sterile pipette tip was used to wound the cell monolayer. Then, a phase-contrast microscope (model IX71; Olympus Corp., Tokyo, Japan) was used to observe the cell migration at 0 h, 24 h and 48 h.

Transwell assay

Cells at a density of 6×10^4 were plated in the upper layer (8 µm; Corning, Lowell, USA). The bottom chamber was filled with medium supplemented with 10% FBS. After 48 h, the cells in the lower chamber were fixed. Then, a crystal violet solution was used to stain cells for further analysis using the microscope (model IX71; Olympus Corp.). Twelve randomly chosen areas per sample were used to assess the number of penetrating cells.

Cell invasion assay

The 2×10^5 cells were plated in the upper chamber of 24-well 8-micrometer pore well chambers (Corning). The cells were covered with diluted BD Matrigel™ (BD Biosciences, Franklin Lakes, USA) containing a complete

medium. The lower chamber was filled with a medium containing 10% FBS. After 24 h, cells on the lower layer were fixed with 4% paraformaldehyde solution and stained with 0.1% crystal violet solution. The total number of penetrating cells was calculated and pictures were taken with a light microscope (model CKX53; Olympus Corp.; ×200 magnification).

Western blot

Total protein was extracted by means of a radioimmunoprecipitation assay (RIPA) buffer supplemented with a mixture of protease and phosphatase inhibitors. The protein concentration was determined with a bicinchoninic acid (BCA) protein assay. Protein samples were separated using 10% sodium dodecyl-sulfate polyacrylamide gel electrophoresis (SDS-PAGE) and transferred to a polyvinylidene fluoride (PVDF) membrane. After blocking with 10% fat-free milk, the membrane was incubated at 4°C overnight with the following primary antibodies: *HIF1α* (1:6000, cat. No. 20960-1-AP), *ROBO1* (1:10000, cat. No. 20219-1-AP), *VEGFC* (1:1000, cat. No. 22601-1-AP), and *SLIT2* (1:600, cat. No. 20217-1-AP; all from ProteinTech Group). Next, the membrane was incubated with horseradish peroxidase (HRP) secondary antibody (1:3000, cat. No. HRP-60004; ProteinTech Group) for 1 h. Chemiluminescent HRP substrate and a suitable X-ray were used to detect the protein bands. Proteins were identified and quantified using the AlphaEaseFC software (Alpha Innotech, San Leandro, USA).

Animal experiments

Male athymic BALB/c mice (5–6 weeks, 16–18 g) were purchased from Nanjing University Animal Laboratory (Nanjing, China). The animals were provided with food and water ad libitum. All experiment conditions conformed to the 3R principles of animal experimentation. To evaluate the role of PIEZO2 in vivo, the mice were injected with SW480 cell suspension ($2{\times}10^6$) in 0.1 mL of culture medium subcutaneously into the right scapular region. The tumor size was measured every 7 days and calculated with the following formula: volume = tumor length × (tumor width)^2 × 0.5236. All data were recorded in millimeters. When the bearing tumors reached ~1 cm^3, mice were killed and tumor samples were weighed and fixed in formalin followed by paraffin embedding.

Immunohistochemistry

In animal experiment, immunohistochemical *Ki-67* staining was used to evaluate the proliferative activity, and *VEGFC* expression was measured to evaluate the effect of *PIEZO2* on angiogenesis in tumor tissues. We also explored the expression of *PIEZO2* in colon cancer samples obtained from the patients of our hospital.

The anti-*Ki67* (cat. No. 27309-1-AP), anti-*PIEZO2* (cat. No. 26205-1-AP) and anti-*VEGFC* (cat. No. 22601-1-AP; all from ProteinTech Group) antibodies were diluted and used at 1:16000, 1:200 and 1:200, respectively. Goat anti-rabbit secondary antibodies were also diluted and used at 1:200, 1:500 and 1:500. The labelling indices were introduced to quantify the expression of *Ki-67* and *VEGFC*, calculated by the ratio of *Ki-67-* and *VEGFC*-positive cells/total cells and quantified using ×200 magnification in 3 randomly selected areas in each tissue sample. We evaluated the *PIEZO2* expression in colon cancer tissues using the staining intensity and staining area of positive tumor cells in each section.[18] The immunohistochemical score was used to assess the expression of *PIEZO2* referred to the protocol described by Tian et al.[19] The median score was used as the split point. The group with values higher than or equal to the median was considered the high-expression group, and the the group with values lower than the median was considered the low-expression group.

TUNEL assay

Tumor tissues were cut into 5-μm-thick slides and the slides were covered with the terminal deoxynucleotidyl transferase dUTP nick end labeling (TUNEL) reaction mixture (cat. No. PF00006; ProteinTech Group). After washing off the unbound enzyme conjugate, a substrate reaction was used to visualize the peroxidase (POD)-retained cells in the immune complex. Using a light microscope (model CKX53; Olympus Corp.) at ×200 magnification, 3 different visual areas of each section were randomly selected and analyzed. The positive rate of apoptotic cells was defined as the density of apoptotic cells (the apoptosis index) using ImageJ software (National Institutes of Health, Bethesda, USA).

Statistical analyses

The relationship between *PIEZO2* expression and the clinical characteristics of gender or site of primary tumor in colon cancer patients was analyzed using Spearman's correlation analysis, and between *PIEZO2* protein expression and the remaining 6 variables using Kendall's tau-b correlation analysis. Comparison between the *PIEZO2* expression in tumor and paired normal tissue samples was performed using χ^2 test. The time from tumor resection to the patient's death or last follow-up was defined as the overall survival (OS) time. The impact of the prognostic role of clinical/pathological characteristics on OS was analyzed using the log-rank test and the Kaplan–Meier analysis. Subsequently, proportional hazard assumption was assessed using Schoenfeld residuals. The variables of N stage and *PIEZO2* did not meet the assumption. The univariate analysis was performed using Cox proportional

hazards regression model for variables that met the assumption. The time-dependent Cox regression model was used for variables that did not meet the assumption. The multivariate analysis was conducted using the time-dependent Cox regression model to exclude the influence of confounding factors. Since the data from the 2 groups met the assumption of normality, the differences between the 2 groups were evaluated using the Student's t-test and expressed with mean ± standard deviation (M ±SD). Because the repeated measurement data from the 2 groups did not show normal distribution, the data of this part were analyzed using the Scheirer–Ray–Hare test and expressed as median ±range. The IBM SPSS v. 20.0 (IBM Corp., Armonk, USA), R v. 4.2.2 software (survminer package; R Foundation for Statistical Computing, Vienna, Austria) and GraphPad Prism v. 9 (GraphPad Software, San Diego, USA) were used in this study. The value of $p < 0.05$ was considered statistically significant.

Results

PIEZO2 expression was increased in colon cancer and associated with poor prognosis

A total of 30 colon cancer specimens with adjacent tissues were randomly selected from patients with colon cancer operated in Second People's Hospital of Lianyungang. The expression of *PIEZO2* was analyzed using immunohistochemistry. The results indicated that *PIEZO2* was mainly located on the cell membrane and cytoplasm (Fig. 1A). The *PIEZO2* was highly expressed in colon cancer tissues compared with normal samples (18/30 compared to 9/30, $\chi^2 = 5.455$, $p = 0.020$; Fig. 1B). As shown in Table 2, high expression of *PIEZO2* was associated with tumor differentiation (Kendall's tau-b = 0.360, $p = 0.002$), T stage (Kendall's tau-b = 0.433, $p < 0.001$), N stage (Kendall's tau-b = 0.453, $p < 0.001$), and clinical stage (Kendall's tau-b = 0.322, $p = 0.006$). In addition, the prognostic data

Fig. 1. A. Immunohistochemical staining images of *PIEZO2* in colon cancer and adjacent colon tissues; B. Difference in expression levels of *PIEZO2* in colon cancer and normal colon samples analyzed using 30 colon cancer patient dataset and χ^2 test; C. The Kaplan–Meier analysis and the log-rank test were used to determine the relationship between the expression of *PIEZO2* and the clinical outcome in 74 colon cancer patients

* $p < 0.05$.

showed that patients with high expression of *PIEZO2* had shorter OS (log-rank (Mantel–Cox) = 15.701, p < 0.001; Fig. 1C). Finally, we found that high expression of *PIEZO2* played an independent prognostic role for worsening OS in colon cancer, as shown with univariate and multivariate analyses (p = 0.007 and p = 0.034, respectively; Table 3).

Suppression of *PIEZO2* decreased the migration and invasion of colon cancer

To explore the potential role of *PIEZO2* in colon cancer, we identified 56 co-expressed genes (Fig. 2A) using the Coexpedia website (http://www.coexpedia.org/index.php). Gene Ontology (GO) function and pathway

enrichment analyses were performed using the DAVID database (https://david.ncifcrf.gov/). As expected, the biological processes were primarily associated with extracellular matrix organization, cellular response to reactive oxygen species (ROS), positive regulation of transcription, templated DNA, and response to hypoxia (Fig. 2B). In terms of cellular components, these genes were also involved in the extracellular matrix (ECM), extracellular space, extracellular region, and receptor complexes (Fig. 2B). The following biological processes were included: ECM structural constituents, integrin binding, ECM binding, collagen binding, and proteoglycan binding (Fig. 2B). In addition, Kyoto Encyclopedia of Genes and Genomes (KEGG) pathway analysis indicated that the following

Table 2. The relationship between *PIEZO2* protein expression and clinical pathological features in colon cancer patients

Characteristic		Total, n	Expression level of *PIEZO2*		p-value
			high	low	
Age [years]	<65 ≥65	30 44	18 27	12 17	0.907
Gender	male female	44 30	25 20	19 10	0.401
Site of primary tumor	left right	31 43	17 28	14 15	0.378
Differentiation	moderate and well poor	37 37	16 29	21 8	0.002
T stage	T1+T2 T3+T4	29 45	10 35	19 10	<0.001
N stage	N0 N1+N2	26 48	8 37	18 11	<0.001
Clinical stage	I II+III	20 54	12 33	8 21	0.006
CEA [ng/mL]	<6 ≥6	19 55	9 36	10 19	0.931

CEA – carcinoembryonic antigen. Spearman's correlation analysis was used to analyze the relationship between the protein expression of *PIEZO2* and the clinical characteristics of gender or site of primary tumor. Kendall's tau-b correlation analysis was applied to explore the relationship between the protein expression of *PIEZO2* and the remaining 6 variables. The value of p < 0.05 was considered statistically significant.

Table 3. Univariate analysis and multivariate analysis of the overall survival (OS) in colon cancer patients

Characteristic	Univariate analysis			Multivariate analysis		
	HR	95% CI	p-value	HR	95% CI	p-value
Age	0.849	0.517–1.393	0.516	0.768	0.416–1.420	0.400
Gender	1.006	0.612–1.653	0.982	0.607	0.318–1.160	0.131
Tumor location	0.806	0.488–1.330	0.398	0.587	0.301–1.144	0.118
Differentiation	2.130	1.299–3.494	0.003	2.652	1.191–5.905	0.017
T stage	1.658	1.004–2.740	0.048	0.367	0.138–0.977	0.045
N stage (time-dependent variable)	3612.754	5.558–2348302.323	0.013	51.028	0.049–52836.422	0.267
Clinical stage	2.350	1.319–4.187	0.004	2.086	1.036–4.202	0.040
PIEZO2 (time-dependent variable)	4261.402	9.758–1861054.007	0.007	1884.388	1.797–1976563.451	0.034
CEA	1.179	0.669–2.077	0.570	1.443	0.729–2.857	0.293

HR – hazard ratio; 95% CI – 95% confidence interval; CEA – carcinoembryonic antigen. Proportional hazard assumption was examined using Schoenfeld residuals. The variables of N stage and *PIEZO2* did not meet the assumption. Subsequently, the univariate analysis was performed using the Cox proportional hazards regression model for the variables that met the assumption. The time-dependent Cox regression model was used for variables that did not meet the assumption. At last, the multivariate analysis was conducted using the time-dependent Cox regression model to exclude the influence of confounding factors. The value of p < 0.05 was considered statistically significant.
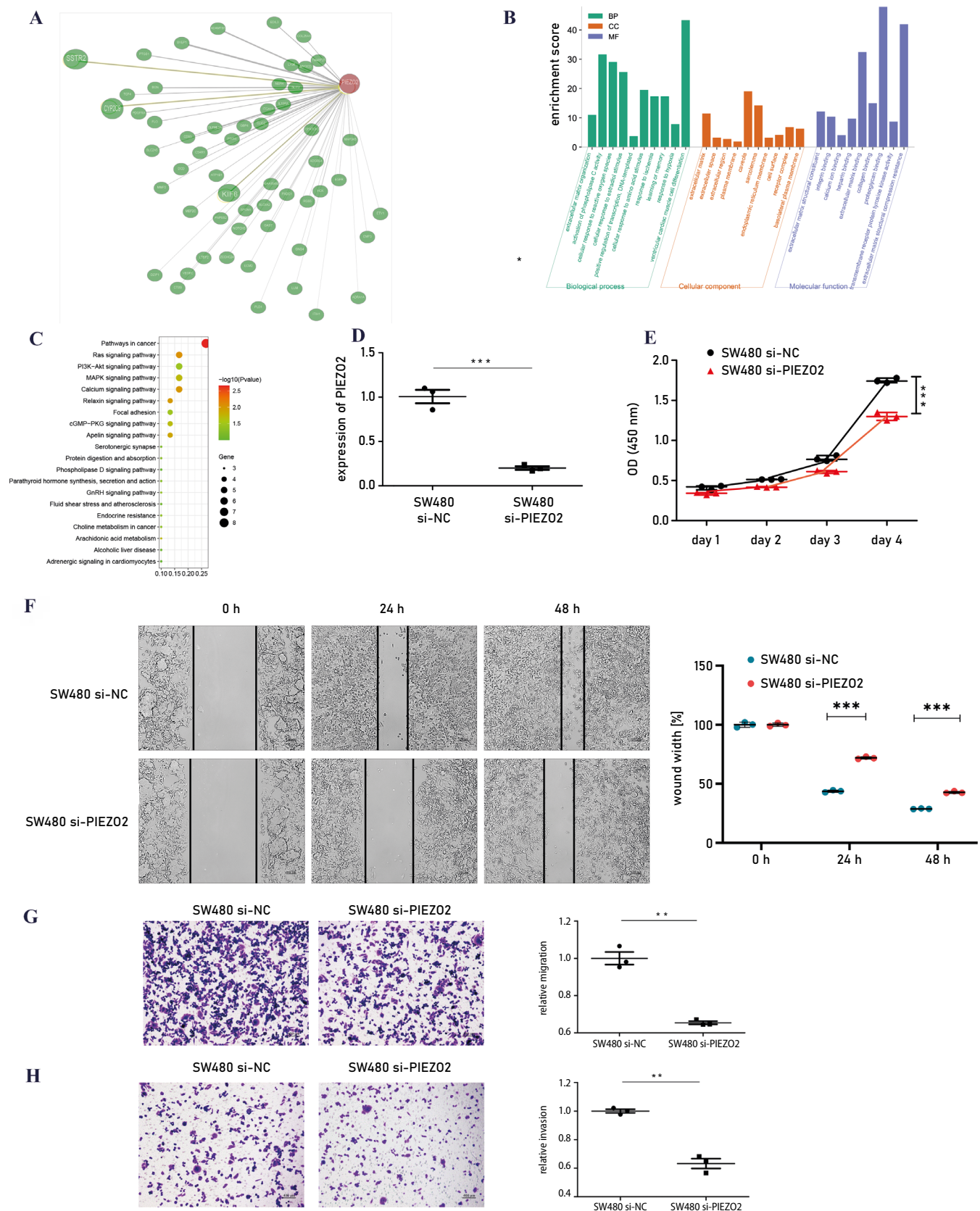
Fig. 2. Inhibition of *PIEZO2* suppresses the proliferation, migration and invasion in colon cancer cells. A. Fifty-six co-expressed genes of *PIEZO2* identified using the Coexpedia website; B. Enrichment analysis of co-expressed genes performed using the DAVID database; C. Kyoto Encyclopedia of Genes and Genomes (KEGG) pathway analysis of co-expressed genes conducted using the DAVID database; D. After the SW480 cells were transfected with small interfering (si)RNA targeting *PIEZO2*, the expression of *PIEZO2* in negative control (NC) and si-*PIEZO2* SW480 cells was tested using quantitative reverse-transcription polymerase chain reaction (qRT-PCR). The results were analyzed using the Student's t-test and expressed with mean ± standard deviation (M ±SD); E. Cell counting kit-8 (CCK-8) assay was performed to evaluate the cell viability of NC and si-*PIEZO2* SW480 cells. The results were analyzed using the Scheirer–Ray–Hare test and expressed as median (range); F,G. Wound healing and cell invasion assays were performed to evaluate the migration ability of NC and si-*PIEZO2* SW480 cells. The results were analyzed using the Student's t-test and expressed as M ±SD; H. Matrigel™ invasion assay was performed to evaluate the invasion ability of NC and si-*PIEZO2* SW480 cells. The results were analyzed using the Student's t-test and expressed as M ±SD. All experiment results were representative of 3 independent experiments

** p < 0.01; *** p < 0.001; OD – optical density.

pathways were enriched in cancer: Ras signaling, PI3K-Akt signaling, MAPK signaling, and calcium signaling pathways (Fig. 2C). As shown in Fig. 2D, a stable transfection with si-*PIEZO2* reduced the mRNA expression of *PIEZO2* in SW480 cells. Moreover, SW480 cells with si-*PIEZO2* showed weaker cell proliferation, migration and invasion functions (Fig. 2E–H).

PIEZO2 is linked to the *SLIT2*/*ROBO1*/*VEGFC* pathway

A previous study suggested that *PIEZO2* plays a pivotal role in tumor angiogenesis.[9] We explored the mRNA expression of *VEGFA*, *VEGFB*, *VEGFC*, and *VEGFD* in control and transfected SW40 cells, and the results indicated that only the expression of *VEGFC* was significantly decreased in si-*PIEZO2* SW480 cells (Fig. 3A). A recent study indicated that *SLIT2*/*ROBO1* signaling participates

in angiogenesis in a pathological context.[20] We analyzed the relationship between *SLIT2*, *ROBO1*, *VEGFC*, *HIF-1α*, and *PIEZO2* using the online website CBioPortal for Cancer Genomics (http://www.cbioportal.org/). The obtained results showed that the mRNA expression of *PIEZO2* is positively correlated with the expression of *VEGFC*, *SLIT2*, *ROBO1*, and HIF-1α (Fig. 3B–E). Furthermore, we assessed the protein and mRNA expression of *VEGFC*, *SLIT2*, *ROBO1*, and *HIF-1α* in control and transfected SW40 cells, and found that *VEGFC*, *SLIT2*, *ROBO1*, and *HIF-1α* were expressed at lower levels in transfected SW40 cells compared to the control SW40 cells (Fig. 3F,G).

Suppression of *PIEZO2* inhibits the growth of colon cancer in vivo

To determine the function of *PIEZO2* in tumor growth, we injected control and transfected SW480 cells
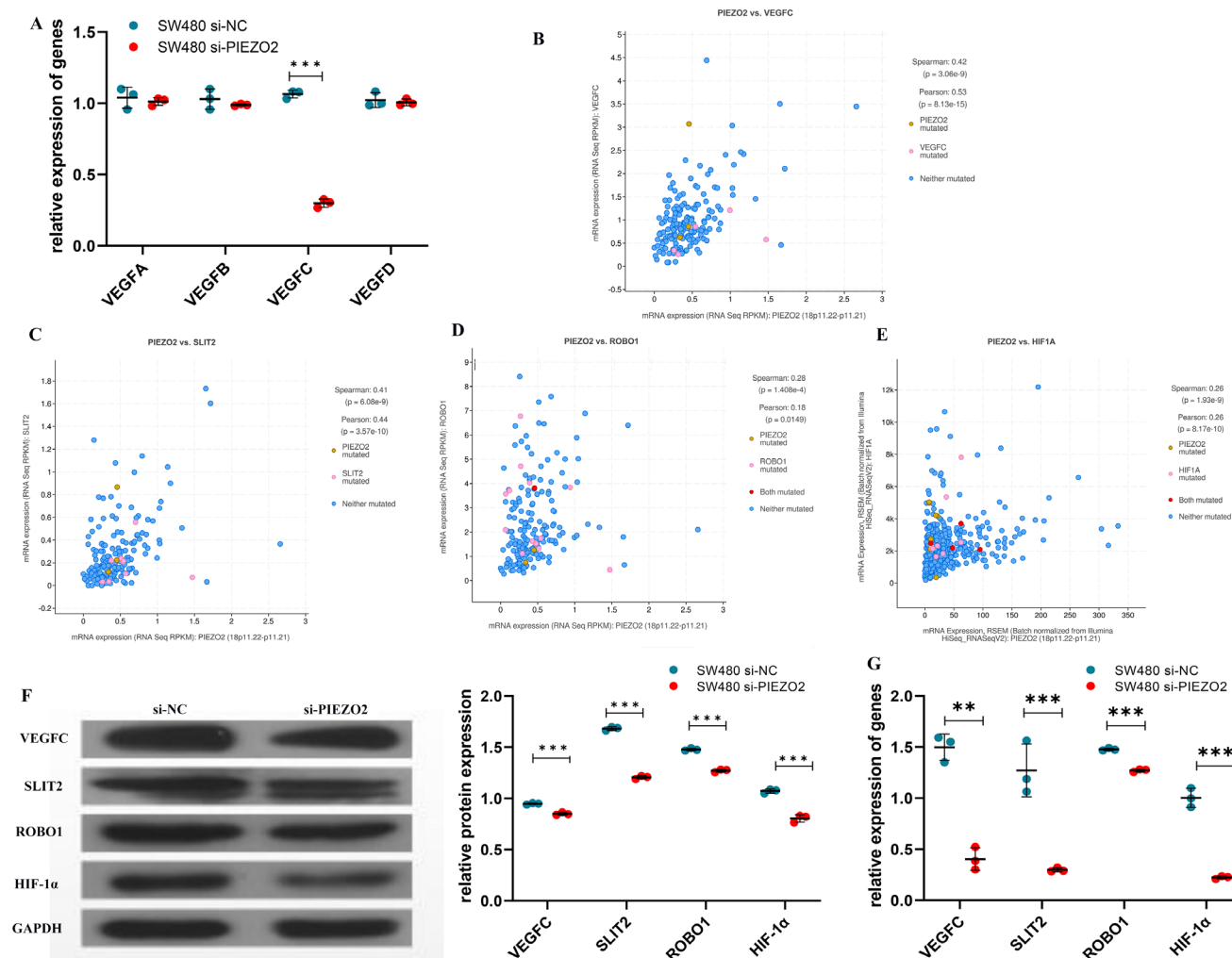

Fig. 3. *PIEZO2* is correlated with the *SLIT2*/*ROBO1*/*VEGFC* pathway. A. The expression of *VEGFA*, *VEGFB*, *VEGFC*, and *VEGFD* in negative control (NC) and si-*PIEZO2* SW480 cells was tested using quantitative reverse-transcription polymerase chain reaction (qRT-PCR). The differences were analyzed using the Student's t-test and expressed with mean ± standard deviation (M ±SD); B–E. Correlation between *PIEZO2* and *VEGFC*, *SLIT2*, *ROBO1*, and *HIF1A* was explored using the website CBioPortal for Cancer Genomics; F,G. The expression of *VEGFC*, *SLIT2*, *ROBO1*, and *HIF1A* in NC and si-*PIEZO2* SW480 cells were tested using western blot and qRT-PCR

** p < 0.01; *** p < 0.001.

subcutaneously into nude mice. As shown in Fig. 4A, tumors in control SW480 cell group grew faster and larger than those in transfected SW480 cell group. Consistent with the tumor volumes, the average tumor weight was clearly reduced (Fig. 4B). Moreover, the transfected SW480 cells showed a reduced expression of *Ki67* compared to the control group (Fig. 4C). Additionally, the group of transfected SW480 cells had a higher apoptosis index of tumor cells than the control group (Fig. 4D). Finally, we detected the expression of *VEGFC* in both groups. The results indicated that *VEGFC* expression in transfected SW480 cells was lower than in the control group (Fig. 4E).

Positive correlation exists between *PIEZO2* expression and cancer-associated fibroblasts

Recent studies have emphasized the role of cancer-associated fibroblasts (CAFs) in cancer progression and immune response. To explore the role of *PIEZO2* in CAFs, we analyzed the correlation between *PIEZO2* expression and CAFs using TIMER 2.0 (http://timer.cistrome.org/), and found that the expression of *PIEZO2* was positively correlated with CAFs in colon cancer (Fig. 5A). Then, we analyzed the expression markers of CAFs in colon cancer and discovered that *PIEZO2* expression was statistically associated with immune subtypes, including wound healing, interferon gamma (IFN-γ) dominant, inflammatory, lymphocyte depleted, and TGF-β dominant (Fig. 5B). Finally, we evaluated the role of *PIEZO2* in CAFs in the tumor immune single-cell hub (TISCH). The results indicated that the *PIEZO2* expression was positively correlated with CAFs in colon cancer (Fig. 5C).

Discussion

Our data provide evidence that *PIEZO2* expression increased in colon cancer and played a negative role in tumor survival. The results demonstrated that *PIEZO2* promoted the proliferation, migration and invasion of colon cancer cells, and the detailed mechanism may be related to the *SLIT2/ROBO1/VEGFC* pathway.

The *PIEZO* channels are a new class of mechanosensitive channels, mainly responsible for the induction to mechanical forces and the entry or exit of Ca^{2+} in cells.[21] The *PIEZO* channels are large transmembrane proteins composed of more than 2500 amino acids and 24–36 putative transmembrane fragments, including *PIEZO1* and *PIEZO2* members. The *PIEZO* channels play an important physiological role in various mechanotransduction processes including touch, hearing and blood pressure perception in mammals. Recent evidence also suggested that *PIEZO1* was necessary for vascular development and function, and lineage choice of neural stem cells.[22] The *PIEZO2* plays an essential role in sensory transmission

such as touch, mechanical proprioception, and gastrointestinal[23,24] and respiratory physiology. Moreover, some studies reported that *PIEZO* family made paramount contributions to the skeletal system, mainly in bone formation and mechanically stimulated bone homeostasis.[25,26]

Mechanosensitive channels are necessary for mechanotransduction and are frequently lodged on the cell surface. Our results also confirmed that *PIEZO2* is mainly expressed on the cell membranes of colon cells. The *PIEZO* channels play an important role in the pathogenesis of various diseases. Mechanical stress promoted stem cell differentiation by *PIEZO* channels in the adult *Drosophila* midgut, and this process was related to increased cytosolic Ca^{2+} levels caused by a direct mechanical stimulus.[27] In fibrotic tissues, mechanical signaling regulated the interactions between cells and the ECM through discoidin domain receptor 1.[28] However, several different cells sensed the stiffness of the surrounding substrate and responded to light by *PIEZOs*.[29] Stiffness may regulate the expression of matricellular protein *CCN1/CYR61* in endothelial cells after the tumor invasion, indicating that stiffness-induced changes are a potential target for impairing tumor metastasis.[30]

Some studies have suggested that *PIEZO2* participates in the occurrence and development of malignant tumors. One study identified high expression of *PIEZO2* in breast cancer and revealed that patients with elevated expression of *PIEZO2* had a favorable prognosis in breast cancer.[31] However, another study reported that the expression of *PIEZO2* was clearly reduced in non-small-cell lung cancer (NSCLC) tissue and high expression of *PIEZO2* correlated with better OS in NSCLC, especially in the adenocarcinoma subgroup.[32] According to a recent study, *PIEZO2* significantly increased in bladder cancer tissue, indicating that *PIEZO2* dysfunction may contribute to the carcinogenesis of bladder cancer by causing proliferative changes and angiogenesis.[10] Our results indicated that *PIEZO2* was highly expressed in colon cancer and correlated with poor prognosis, which is consistent with previous results.

As far as we know, when solid tumors grow beyond a certain size, they require angiogenesis to supply nutrients. In this process, some inflammatory and cell factors are involved.[33] Yang et al. reported that *PIEZO2* increased angiogenesis and vascular hyperpermeability in endothelial cells, and $Ca^{2+}/Wnt11/β\text{-}catenin$ signaling played an important role in this process.[9] Another study suggested that intracellular Ca^{2+} signaling promoted angiogenesis and vasculogenesis by enhancing the functions of vascular endothelial cells (VECs) and endothelial colony-forming cells, which is linked to an increase in the expression of *PIEZO2*.[34] Therefore, these studies indicate that *PIEZO2* is involved in angiogenesis. In this study, we found that the expression of *VEGFC* was changing along with *PIEZO2* expression, which was verified by the level of mRNA, protein and in vivo studies. The *VEGFC* is a member of *VEGF* family and plays an important role in lymphangiogenesis. The *VEGFC* stimulates the formation of new lymph vessels and provides
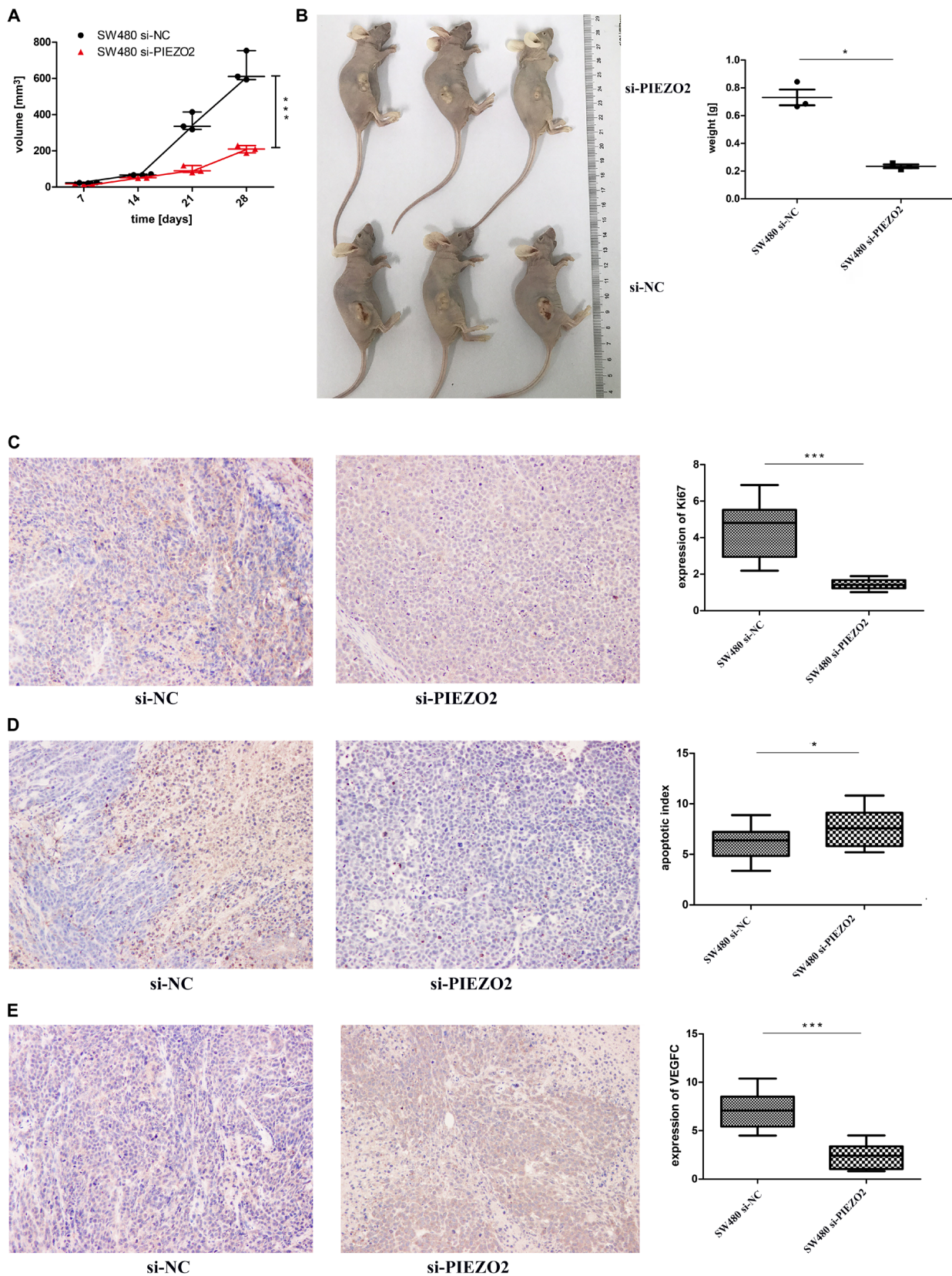
Fig. 4. Suppression of *PIEZO2* significantly inhibits the growth of colon cancer in vivo. The negative control (NC) or si-*PIEZO2* SW480 cells (2×10^6) in 0.1 mL of culture medium were injected subcutaneously into the right scapular region of nude mice to evaluate the antitumor activity of *PIEZO2* in vivo (3 mice per group). The tumor size was measured every 7 days using the formula A×B^2×0.5236, where A is the length and B is the width of the tumor; all measurements were recorded in millimeters. When the bearing tumors were approx. 1 cm^3 in size, all mice were sacrificed, and tissue specimens were weighed and fixed in formalin for paraffin embedding. A. Tumor volumes were measured every 7 days using caliper measurements. The differences between the 2 groups were compared using the Scheirer–Ray–Hare test and expressed as median (range); B. The difference in tumor weight between the 2 groups was analyzed using the Student's t-test and expressed as mean ± standard deviation (M ±SD); C. Proliferation analysis of tumor tissues was performed using *Ki67* immunohistochemical staining, and the difference between the 2 groups was evaluated using the Student's t-test and expressed as M ±SD; D. Apoptosis analysis of tumor tissues was performed using the terminal deoxynucleotidyl transferase dUTP nick end labeling (TUNEL) assay. The differences between the 2 groups were compared using the Student's t-test and expressed as M ±SD; E. *VEGFC* expression was tested with immunohistochemical staining. The differences between the 2 groups were compared using the Student's t-test and expressed as M ±SD
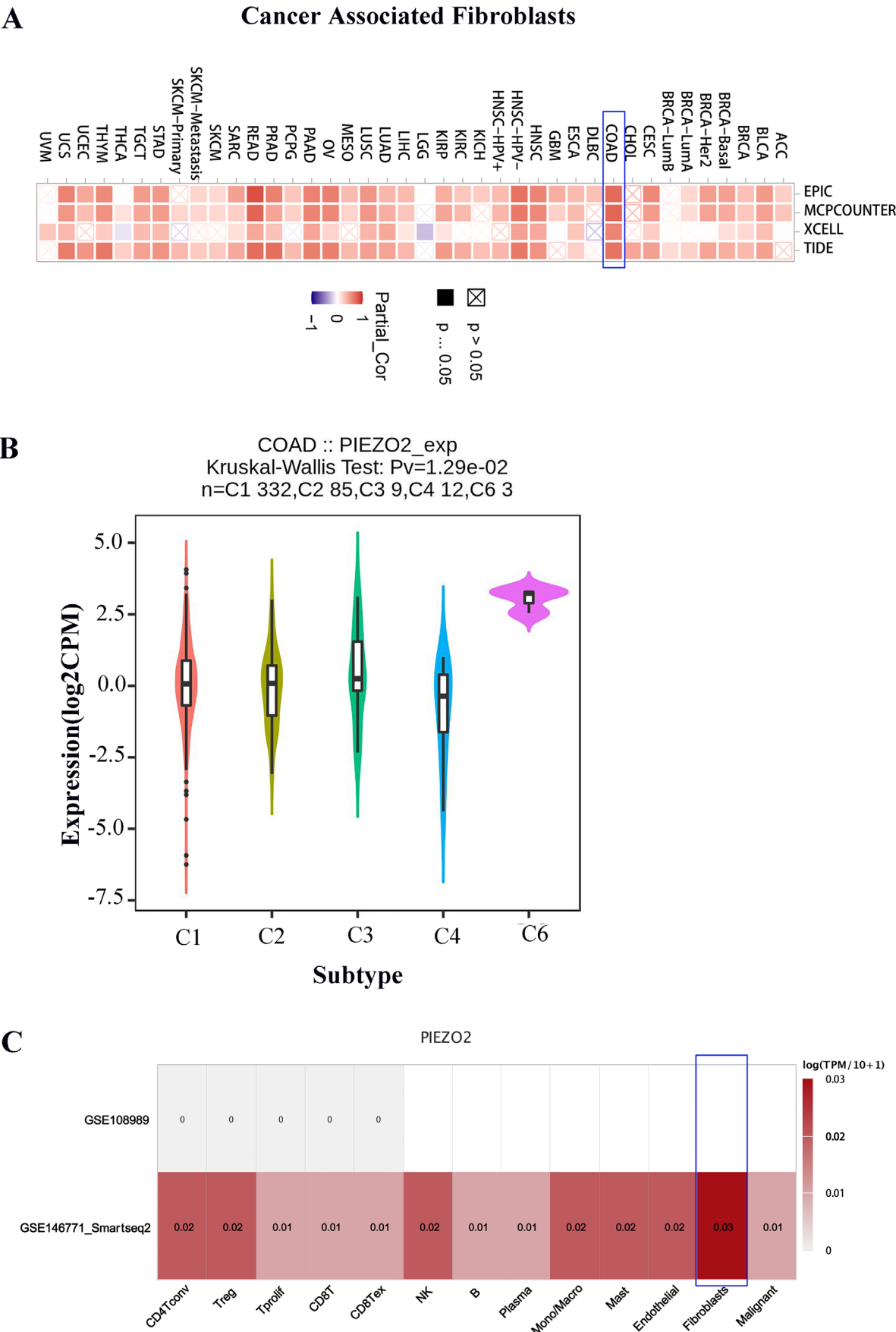
* $p < 0.05$; *** $p < 0.001$.

Fig. 5. Positive correlation between *PIEZO2* expression and cancer-associated fibroblasts (CAFs). A. *PIEZO2* expression level in immune subtypes in colon adenocarcinoma (COAD) based on tumor-immune system interactions database (TISIDB) (http://cis.hku.hk/TISIDB/); C. Correlation between *PIEZO2* expression in single-cell sequencing and CAFs using the tumor immune single-cell hub (TISCH)

a chance for detached cancer cells to metastasize to a distant site.[35] The *VEGFC* can promote the immune escape in colon cancer by activating *VEGFR3*, which results in tumor growth.[36] Moreover, our results suggest that *PIEZO2* is linked to the *SLIT2/ROBO1* pathway. Additionally, some studies reported that the *SLIT2/ROBO1* signaling participates in the process of angiogenesis.[20,37] Overall, our results suggest that *PIEZO2* plays an antiangiogenic role through the *SLIT2/ROBO1/VEGFC* pathway. However, the detailed mechanism is needed to be explored further.

Currently, the tumor microenvironment (TME) is a trending topic in tumor research. Among numerous components of TME, CAFs play an important role in regulating tumorigenesis. Affo et al. found that a pan-CAF signature was significantly associated with poor survival in cholangiocarcinoma and tumor recurrence.[38] Another study found that when pancreatic cancer cells were co-cultured with CAFs, cancer stemness increased.[39] A recent study suggested that CAFs are the primary source of TIMP-1, and TIMP-1 production is enhanced through cancer–stromal interaction, which promotes cancer cell migration.[40] Regarding colon cancer, one study suggested that increased *RAB31* expression in CAFs may contribute to tumor progression by regulating hepatocyte growth factor (HGF) secretion in the tumor stoma.[41] Our study showed that the expression of *PIEZO2* positively correlates with CAFs in colon cancer, indicating that *PIEZO2* is a prognostic factor of the disease. Recently, 6 immune subtypes were identified by immunogenomic data from 33 different types of cancer.[42] This classification method can distinguish the beneficiaries of immune targeted therapy from multiple heterogeneous tumors. In this study, *PIEZO2* was significantly and aberrantly expressed in C1, C2, C3, C4, and C6 of colon cancer, suggesting that *PIEZO2* might have potential in cancer immune therapy. Moreover, the positive correlation between *PIEZO2* expression and CAFs was further validated using a single-cell sequencing dataset. However, the underlying mechanism of *PIEZO2* regulating CAFs requires further study.

Limitations

There are some shortcomings of our study that are worth considering. First, the sample size of clinical patients was relatively small. A large sample study would be needed to validate the results of our study. Second, the detailed mechanism of *PIEZO2* regulating *SLIT2/ROBO1/VEGFC* pathway had not been explored. This may be the direction of our further research.

Conclusions

The *PIEZO2* is highly expressed and is a poor prognostic factor in colon cancer. Moreover, *PIEZO2* can promote cell proliferation and mobility in colon carcinoma through the *SLIT2/ROBO1/VEGFC* pathway. At the same time, *PIEZO2* is positively correlated with CAFs, indicating that it plays an important role in the CAF function. Therefore, *PIEZO2* may be a potential target for colon cancer treatment.

Supplementary data

The supplementary files are available at https://doi.org/10.5281/zenodo.7428254. The package contains the following files:

Supplementary Table 1. Results of χ^2 phi test for Fig. 1B.

Supplementary Table 2. Results of the log-rank test for Fig. 1C.

Supplementary Table 3. Results of the normality test for Fig. 2D.

Supplementary Table 4. Results of the Student's t-test for Fig. 2D.

Supplementary Table 5. Results of the normality test for Fig. 2E.

Supplementary Table 6. Results of the Scheirer–Ray–Hare test for Fig. 2E.

Supplementary Table 7. Results of the normality test for Fig. 2F.

Supplementary Table 8. Results of the Student's t-test for Fig. 2F.

Supplementary Table 9. Results of the normality test for Fig. 2G.

Supplementary Table 10. Results of the Student's t-test for Fig. 2G.

Supplementary Table 11. Results of the normality test for Fig. 2H.

Supplementary Table 12. Results of the Student's t-test for Fig. 2H.

Supplementary Table 13. Results of the normality test for Fig. 3A.

Supplementary Table 14. Results of the Student's t-test for Fig. 3A.

Supplementary Table 15. Results of the normality test for Fig. 3F.

Supplementary Table 16. Results of the Student's t-test for Fig. 3F.

Supplementary Table 17. Results of the normality test for Fig. 3G.

Supplementary Table 18. Results of the Student's t-test for Fig. 3G.

Supplementary Table 19. Results of the normality test for Fig. 4A.

Supplementary Table 20. Results of the Scheirer–Ray–Hare test Fig. 4A.

Supplementary Table 21. Results of the normality test for Fig. 4B.

Supplementary Table 22. Results of the Student's t-test for Fig. 4B.

Supplementary Table 23. Results of the normality test for Fig. 4C.

Supplementary Table 24. Results of the Student's t-test for Fig. 4C.

Supplementary Table 25. Results of the normality test for Fig. 4D.

Supplementary Table 26. Results of the Student's t-test for Fig. 4D.

Supplementary Table 27. Results of the normality test for Fig. 4E.

Supplementary Table 28. Results of the Student's t-test for Fig. 4E.

Supplementary Table 29. Results of Spearman's correlation analysis for Table 2.

Supplementary Table 30. Results of Kendall's tau-b correlation analysis for Table 2.

Supplementary Table 31. Results of Schoenfeld residuals for Table 3.

Supplementary Table 32. Results of the univariate analysis for Table 3.

Supplementary Table 33. Results of the multivariate analysis for Table 3.

ORCID iDs

Haotian Shang https://orcid.org/0000-0002-5057-5924
Aiguo Xu https://orcid.org/0000-0002-1131-7391
Haicui Yan https://orcid.org/0000-0002-4644-6628
Dandan Xu https://orcid.org/0000-0002-2555-9279
Jingyu Zhang https://orcid.org/0000-0002-8381-2973
Xinjian Fang https://orcid.org/0000-0002-0366-5521

References

1. Sung H, Ferlay J, Siegel RL, et al. Global cancer statistics 2020: GLOBOCAN estimates of incidence and mortality worldwide for 36 cancers in 185 countries. *CA Cancer J Clin*. 2021;71(3):209–249. doi:10.3322/caac.21660

2. Lee RM, Cardona K, Russell MC. Historical perspective: Two decades of progress in treating metastatic colorectal cancer. *J Surg Oncol*. 2019;119(5):549–563. doi:10.1002/jso.25431

3. Willyard C. Cancer therapy: An evolved approach. *Nature*. 2016;532(7598):166–168. doi:10.1038/532166a

4. De Felice D, Alaimo A. Mechanosensitive piezo channels in cancer: Focus on altered calcium signaling in cancer cells and in tumor progression. *Cancers (Basel)*. 2020;12(7):1780. doi:10.3390/cancers12071780

5. Martino F, Perestrelo AR, Vinarský V, Pagliari S, Forte G. Cellular mechanotransduction: From tension to function. *Front Physiol*. 2018;9:824. doi:10.3389/fphys.2018.00824

6. Coste B, Xiao B, Santos JS, et al. Piezo proteins are pore-forming subunits of mechanically activated channels. *Nature*. 2012;483(7388):176–181. doi:10.1038/nature10812

7. Gottlieb PA, Bae C, Sachs F. Gating the mechanical channel Piezo1: A comparison between whole-cell and patch recording. *Channels*. 2012;6(4):282–289. doi:10.4161/chan.21064

8. Yang XN, Lu YP, Liu JJ, et al. Piezo1 is a novel trefoil factor family 1 binding protein that promotes gastric cancer cell mobility in vitro. *Dig Dis Sci*. 2014;59(7):1428–1435. doi:10.1007/s10620-014-3044-3

9. Yang H, Liu C, Zhou RM, et al. Piezo2 protein: A novel regulator of tumor angiogenesis and hyperpermeability. *Oncotarget*. 2016;7(28):44630–44643. doi:10.18632/oncotarget.10134

10. Etem E, Ceylan G, Özaydın S, Ceylan C, Özercan I, Kuloğlu T. The increased expression of Piezo1 and Piezo2 ion channels in human and mouse bladder carcinoma. *Adv Clin Exp Med*. 2018;27(8):1025–1031. doi:10.17219/acem/71080

11. Chen X, Wanggou S, Bodalia A, et al. A feedforward mechanism mediated by mechanosensitive ion channel PIEZO1 and tissue mechanics promotes glioma aggression. *Neuron*. 2018;100(4):799.e7–815.e7. doi:10.1016/j.neuron.2018.09.046

12. Pardo-Pastor C, Rubio-Moscardo F, Vogel-González M, et al. Piezo2 channel regulates RhoA and actin cytoskeleton to promote cell mechanobiological responses. *Proc Natl Acad Sci U S A*. 2018;115(8):1925–1930. doi:10.1073/pnas.1718177115

13. Mertsch S, Schmitz N, Jeibmann A, Geng JG, Paulus W, Senner V. Slit2 involvement in glioma cell migration is mediated by Robo1 receptor. *J Neurooncol*. 2008;87(1):1–7. doi:10.1007/s11060-007-9484-2

14. Xia Y, Wang L, Xu Z, et al. Reduced USP33 expression in gastric cancer decreases inhibitory effects of Slit2-Robo1 signaling on cell migration and EMT. *Cell Prolif*. 2019;52(3):e12606. doi:10.1111/cpr.12606

15. Ahirwar DK, Peng B, Charan M, et al. Slit2/Robo1 signaling inhibits small cell lung cancer by targeting β-catenin signaling in tumor cells and macrophages [published online as ahead of print on July 15, 2022]. *Mol Oncol*. 2022. doi:10.1002/1878-0261.13289

16. Yao Y, Zhou Z, Li L, et al. Activation of Slit2/Robo1 signaling promotes tumor metastasis in colorectal carcinoma through activation of the TGF-β/Smads pathway. *Cells*. 2019;8(6):635. doi:10.3390/cells8060635

17. Tan Q, Liang XJ, Lin SM, et al. Engagement of Robo1 by Slit2 induces formation of a trimeric complex consisting of Src-Robo1-E-cadherin for E-cadherin phosphorylation and epithelial-mesenchymal transition. *Biochem Biophys Res Commun*. 2020;522(3):757–762. doi:10.1016/j.bbrc.2019.11.150

18. Gu Y, Li X, Bi Y, et al. CCL14 is a prognostic biomarker and correlates with immune infiltrates in hepatocellular carcinoma. *Aging*. 2020;12(1):784–807. doi:10.18632/aging.102656

19. Tian Y, Zhou Y, Liu J, et al. Correlation of SIDT1 with poor prognosis and immune infiltration in patients with non-small cell lung cancer. *Int J Gen Med*. 2022;15:803–816. doi:10.2147/IJGM.S347171

20. Liu J, Hou W, Guan T, et al. Slit2/Robo1 signaling is involved in angiogenesis of glomerular endothelial cells exposed to a diabetic-like environment. *Angiogenesis*. 2018;21(2):237–249. doi:10.1007/s10456-017-9592-3

21. Xu XZS. Demystifying mechanosensitive piezo ion channels. *Neurosci Bull*. 2016;32(3):307–309. doi:10.1007/s12264-016-0033-x

22. Qin L, He T, Chen S, et al. Roles of mechanosensitive channel Piezo1/2 proteins in skeleton and other tissues. *Bone Res*. 2021;9(1):44. doi:10.1038/s41413-021-00168-8

23. Bai T, Li Y, Xia J, et al. Piezo2: A candidate biomarker for visceral hypersensitivity in irritable bowel syndrome? *J Neurogastroenterol Motil*. 2017;23(3):453–463. doi:10.5056/jnm16114

24. Wang F, Knutson K, Alcaino C, et al. Mechanosensitive ion channel Piezo2 is important for enterochromaffin cell response to mechanical forces: Piezo2 in EC cells. *J Physiol*. 2017;595(1):79–91. doi:10.1113/JP272718

25. Zhou T, Gao B, Fan Y, et al. Piezo1/2 mediate mechanotransduction essential for bone formation through concerted activation of NFAT-YAP1-ß-catenin. *eLife*. 2020;9:e52779. doi:10.7554/eLife.52779

26. Wang L, You X, Lotinun S, Zhang L, Wu N, Zou W. Mechanical sensing protein PIEZO1 regulates bone homeostasis via osteoblast-osteoclast crosstalk. *Nat Commun*. 2020;11(1):282. doi:10.1038/s41467-019-14146-6

27. He L, Si G, Huang J, Samuel ADT, Perrimon N. Mechanical regulation of stem-cell differentiation by the stretch-activated Piezo channel. *Nature*. 2018;555(7694):103–106. doi:10.1038/nature25744

28. Coelho NM, McCulloch CA. Mechanical signaling through the discoidin domain receptor 1 plays a central role in tissue fibrosis. *Cell Adh Migr*. 2018;12(4):348–362. doi:10.1080/19336918.2018.1448353

29. Gottlieb PA. A tour de force: The discovery, properties and function of piezo channels. *Curr Top Membr*. 2017;79:1–36. doi:10.1016/bs.ctm.2016.11.007

30. Reid SE, Kay EJ, Neilson LJ, et al. Tumor matrix stiffness promotes metastatic cancer cell interaction with the endothelium. *EMBO J*. 2017;36(16):2373–2389. doi:10.15252/embj.201694912

31. Lou W, Liu J, Ding B, et al. Five miRNAs-mediated PIEZO2 downregulation, accompanied with activation of Hedgehog signaling pathway, predicts poor prognosis of breast cancer. *Aging*. 2019;11(9):2628–2652. doi:10.18632/aging.101934

32. Huang Z, Sun Z, Zhang X, et al. Loss of stretch-activated channels, PIEZOs, accelerates non-small cell lung cancer progression and cell migration. *Biosci Rep*. 2019;39(3):BSR20181679. doi:10.1042/BSR20181679

33. Carmeliet P, Jain RK. Molecular mechanisms and clinical applications of angiogenesis. *Nature*. 2011;473(7347):298–307. doi:10.1038/nature10144

34. Moccia F. Endothelial Ca2$^+$ signaling and the resistance to anticancer treatments: Partners in crime. *Int J Mol Sci*. 2018;19(1):217. doi:10.3390/ijms19010217

35. Ellis LM, Hicklin DJ. VEGF-targeted therapy: Mechanisms of anti-tumour activity. *Nat Rev Cancer*. 2008;8(8):579–591. doi:10.1038/nrc2403

36. Tacconi C, Ungaro F, Correale C, et al. Activation of the VEGFC/VEGFR3 pathway induces tumor immune escape in colorectal cancer. *Cancer Res*. 2019;79(16):4196–4210. doi:10.1158/0008-5472.CAN-18-3657

37. Romano E, Manetti M, Rosa I, et al. Slit2/Robo4 axis may contribute to endothelial cell dysfunction and angiogenesis disturbance in systemic sclerosis. *Ann Rheum Dis*. 2018;77(11):1665–1674. doi:10.1136/annrheumdis-2018-213239

38. Affo S, Nair A, Brundu F, et al. Promotion of cholangiocarcinoma growth by diverse cancer-associated fibroblast subpopulations. *Cancer Cell*. 2021;39(6):883. doi:10.1016/j.ccell.2021.03.012

39. Nallasamy P, Nimmakayala RK, Karmakar S, et al. Pancreatic tumor microenvironment factor promotes cancer stemness via SPP1–CD44 axis. *Gastroenterology*. 2021;161(6):1998.e7–2013.e7. doi:10.1053/j.gastro.2021.08.023

40. Nakai N, Hara M, Takahashi H, et al. Cancer cell-induced tissue inhibitor of metalloproteinase-1 secretion by cancer-associated fibroblasts promotes cancer cell migration. *Oncol Rep*. 2022;47(6):112. doi:10.3892/or.2022.8323

41. Yang T, Zhiheng H, Zhanhuai W, et al. Increased RAB31 expression in cancer-associated fibroblasts promotes colon cancer progression through HGF-MET signaling. *Front Oncol*. 2020;10:1747. doi:10.3389/fonc.2020.01747

42. Thorsson V, Gibbs DL, Brown SD, et al. The immune landscape of cancer. *Immunity*. 2018;48(4):812.e14–830.e14. doi:10.1016/j.immuni.2018.03.023